

INCREASE IN IONIC CONDUCTIVITY IN THE NANOCRYSTALLINE PHASE $\text{NaBi}(\text{MoO}_4)_2:\text{Gd}^{3+}$

Bilal Abu Sal^{1*}, Khalil J. Hamam¹, V. M. Moiseyenko², O. V. Ohienko², M. P. Derhachov²

¹*Tafila Technical University, Tafila, Jordan*

²*Oles Honchar Dnipro National University, Dnipro, Ukraine.*

e-mail: bilal_abu@hotmail.com

Nanocomposite based on synthetic opal soaked with the $\text{NaBi}(\text{MoO}_4)_2:\text{Gd}^{3+}$ melt was characterized by X-ray diffraction patterns and Raman spectroscopy technique. Crystalline state of the substance inside opal pores was proved for the composite. The angular positions and intensities of reflections in X-ray diffractograms were different for nanocrystals compared to the crystal. Raman spectrum of opal – $\text{NaBi}(\text{MoO}_4)_2:\text{Gd}^{3+}$ was not essentially changed compared to that of the single crystal, except for a shift of some Raman bands. The total conductivity of nanocrystals was measured in the frequency range from 1 Hz to 1MHz and temperature range from 290 K to 473 K. Impedance hodographs (Nyquist plots) for nanocomposite were plotted. The energy of activation of conductivity and the nature of its frequency dependence were determined. Hopping conduction mechanism was established. The comparison of the temperature dependence with theory made it possible to estimate the average size of nanocrystals in opal pores.

Keywords: nanocomposite, nanomaterials, photonic crystals, synthetic opal, Raman spectroscopy, ionic conductivity.

Received 08.11.2021; Received in revised form 09.12.2021; Accepted 10.12.2021

1. Introduction

The creation and study of the physical properties of new nanomaterials based on synthetic opals and active dielectric crystals is of fundamental interest from the point of view of the physics of low-dimensional systems. Synthetic opals are three-dimensional structures consisting of close-packed monodisperse silica globules that form an fcc lattice. Such structures have tetrahedral and octahedral pores, which are connected with channels. Typical values of the globule diameter and the linear size of the pores are hundreds and tens of nanometers, respectively. The pores can be filled with various materials using various techniques. A method based on a melt is promising for filling the opal pores with active dielectrics. Using this method, you can create 3D-periodic structures of nanocrystals of active dielectrics formed in pores of the opal matrix [1-3]. The unique physical properties of dielectric nanocrystals are due to size effects, which are caused by the increasing role of the surface with a decrease in size to less than 100 nm. In this case, the structure and properties of the surface of nanocrystals are radically different from the properties in the bulk of the crystal due to surface structural relaxation [4]. In [5], within the framework of the model of surface tension in nanoparticles, it was found that the activation energy of ionic conductivity decreases with decreasing nanoparticle size, while the conductivity increases. The revealed theoretically regularities are confirmed by the results of measurements of the temperature and size dependences of the conductivity of oxygen ions in nanograined ceramics $\text{ZrO}_2:16\% \text{ Y}$ [6].

The aim of this work was to study the regularities of the temperature-frequency dependence of the electrical conductivity of $\text{NaBi}(\text{MoO}_4)_2:\text{Gd}^{3+}$ nanocrystals in the opal matrix pores by impedance spectroscopy.

Single crystals of $\text{NaBi}(\text{MoO}_4)_2$ doped with rare-earth metal ions are promising materials for solid lasers and require comprehensive study. The crystals are disordered in the distribution of Na^+ and Bi^{3+} ions in two nonequivalent type positions, while gadolinium ions Gd^{3+} occupy the position of bismuth [7]. Earlier, the study of the total conductivity in alternating fields in bulk single crystals of $\text{NaBi}(\text{MoO}_4)_2$ was carried out in [8], in which it was concluded that the hopping mechanism of conductivity existed in such material.

2. Experimental

Original synthetic opals were grown by natural sedimentation of monodisperse SiO_2 spheres synthesized by using the modified Stober technique [1, 9]. $\text{NaBi}(\text{MoO}_4)_2:\text{Gd}^{3+}$ single crystal was grown by the Czochralski technique [10]. The filling of the opal sample pores was carried out by their impregnation with a melt of a single crystal ($T_m = 1133 \text{ K}$) under the action of capillary forces [1]. The fact of the melt entering the opal pores was recorded by the shift of the Bragg reflection band maximum to the long-wavelength region. Additionally, the Raman spectra of the nanocomposite opal – $\text{NaBi}(\text{MoO}_4)_2:\text{Gd}^{3+}$ were measured. The Raman spectrum of opal – $\text{NaBi}(\text{MoO}_4)_2:\text{Gd}^{3+}$ was not essentially changed compared to that of the single crystal [11], except for a shift of some Raman bands.

3. Results and discussion

X-ray diffractograms (XRD) of opal- $\text{NaBi}(\text{MoO}_4)_2:\text{Gd}^{3+}$ nanocomposite and polycrystalline powder of $\text{NaBi}(\text{MoO}_4)_2:\text{Gd}^{3+}$ were measured (shown in Fig. 1). XRD pattern of synthetic opals were presented in the work [12].

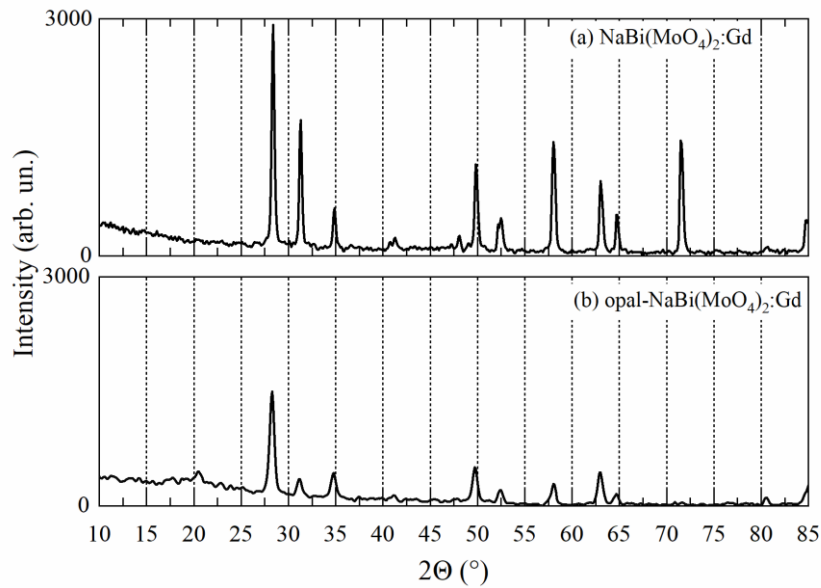


Fig. 1. X-ray diffraction patterns.

As can be seen from the Fig. 1, the angular positions of the diffraction maxima for the opal- $\text{NaBi}(\text{MoO}_4)_2:\text{Gd}^{3+}$ nanocomposite coincide with the data for the bulk monocrystal within the measurement accuracy ($\pm 0.1^\circ$). However, the intensities and half-widths of the reflexes differ. It is known that a decrease in the size of crystallites causes diffraction lines broadening and that the integral width of the diffraction line profile is inversely proportional to the size of crystallites in the sample [13]. The broadening due to the particle size distribution is determined by the expression:

$$\beta = \lambda / D \cos \theta, \quad (1)$$

where D is the effective size of the nanocrystal. Thus, broader diffraction peaks in the nanocomposite may indicate the presence of a nanocrystalline phase in the sample opal- $\text{NaBi}(\text{MoO}_4)_2:\text{Gd}^{3+}$ nanocomposite.

The powder of the composite was compressed into circular pellets (10 mm diameter and 1mm thickness) under 10 tons (1MPa) using a hydraulic press at room temperature.

Both faces of the pellets were silvered to reduce possible surface current and achieve a good conductivity.

The real and imaginary components of the complex impedance as well as the phase shift were measured in the frequency range from 1 Hz to 1 MHz and temperature range from 290 K to 390 K using Solartron-1260 Impedance / Gain Phase Analyzer with 1294 Dielectric Interface, UK. The applied voltage signal has an amplitude of 0.2 V with an accuracy of 0.1%. The real and imaginary components of the complex impedance as well as the phase shift were measured in the frequency range from 1 Hz to 1 MHz and temperature range from 363 K to 473 K using LCR meter from Hioki. The applied voltage signal had an amplitude of 0.5 V. The temperature dependence measurements were taken inside an oven, under ambient atmospheric conditions.

The impedance spectra (Nyquist plots) indicate the semiconductor behavior of the material (bulk resistance decrease with temperature increasing). The bulk conductivity was given by $\sigma_b = t/RA$, where A is the area of the electrodes, t is the thickness of the sample, and R is the bulk resistance (determined from the diameter of the semicircle). Fig. 2 shows that bulk conductivity (σ_b) has a temperature dependence and can be described by an Arrhenius equation:

$$\sigma_b = \sigma_o \exp\left(\frac{-E_b}{k_B T}\right), \quad (2)$$

where σ_o is the pre-exponent factor, E_b is the activation energy, and T is the absolute temperature and k_B is Boltzmann constant ($8.61 \times 10^{-5} \text{ eV K}^{-1}$). The calculated value of the bulk activation energy is $E_b = 0.17 \text{ eV}$.

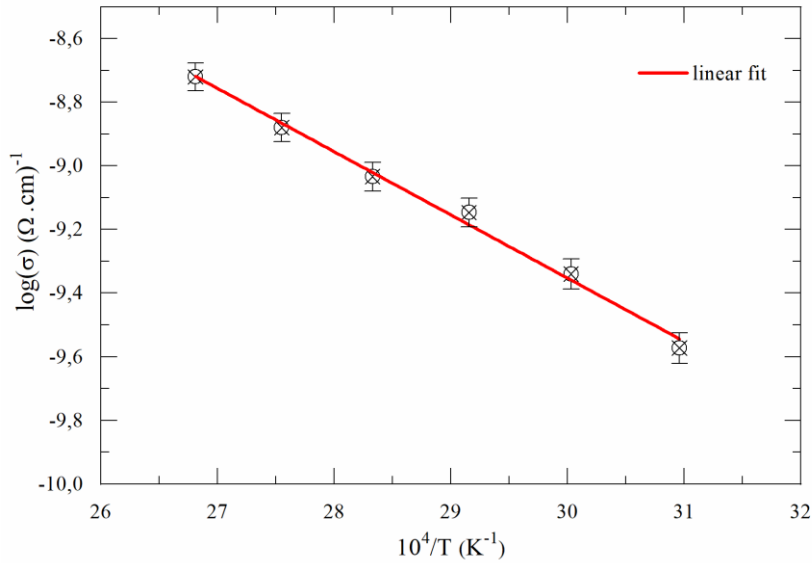


Fig. 2. Bulk conductivity as a function of temperature.

The type of conduction mechanism in the material can be determined by studying the frequency dependence of conductivity (σ_{ac}). σ_{ac} is usually expressed within the framework of the Jonscher universal power law (JPL) $\sigma_{ac} = A \omega^n$ [14] where A is a temperature dependent parameter, n is the exponent factor. Fig. 3 shows the temperature dependence of the exponent factor (n) where n is decreasing as the temperature increases. Such behavior of n and its recorded values ($n < 1$) make the correlated barrier hopping (CBH) model as proposed by Elliot [15] to be the most suitable model for describing the conduction mechanism inside of our present material.

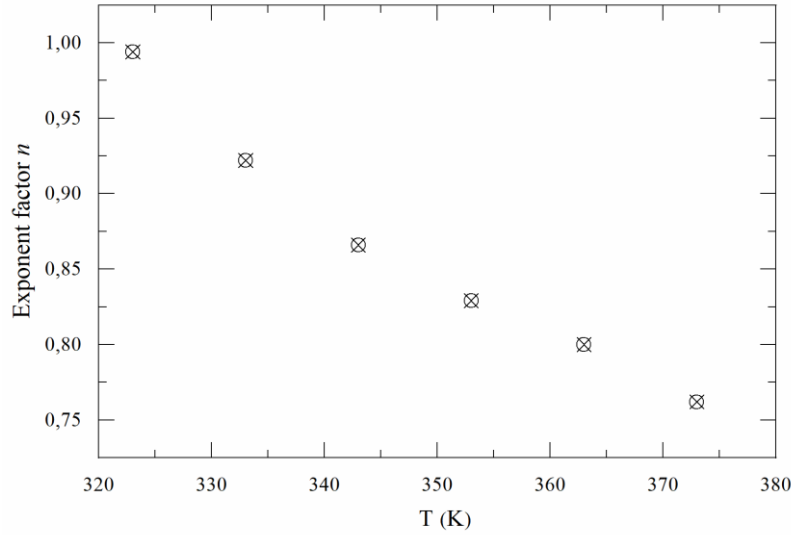


Fig. 3. The exponent factor of ac conductivity.

The temperature dependence of bulk conductivity from 363 K to 473 K are shown in Fig. 4.

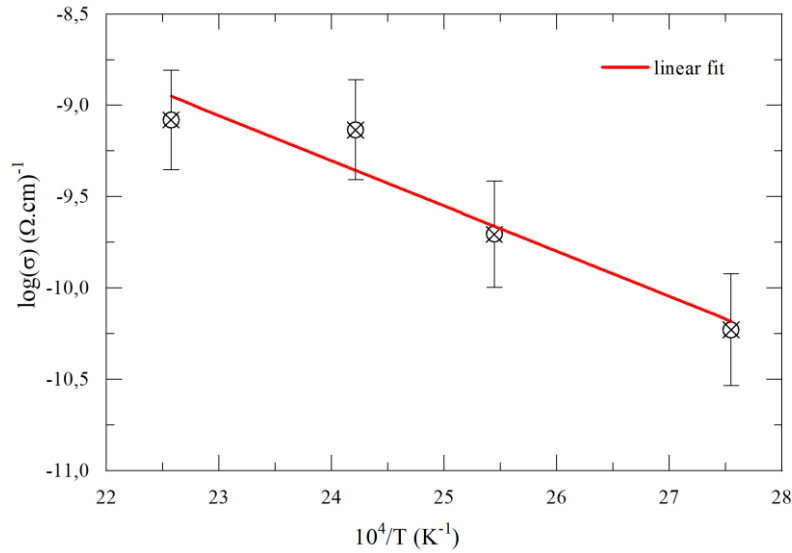


Fig. 4. Bulk conductivity as a function of temperature.

At high temperature the calculated value of the bulk activation energy is $E_b = 0.213$ eV. Fig. 5 shows the temperature dependence of the factor (n) at frequency higher than 10^4 Hz, where n is decreasing as the temperature increases.

The theoretical dependence of the ionic conductivity was calculated using the formula from [5] assuming that the main contribution to the conductivity is made by Na^+ ions:

$$\frac{I_0}{A} \approx \exp\left(-\frac{E_0}{kT}\right) \sinh\left(\frac{2\alpha V}{R_0 kT}\right) \quad (3)$$

The following values were used as initial parameters: $E_0 = 1.2$ eV [8], the volume of the sodium ion $V = 3.94 \times 10^{-3}$ nm³. A comparison of theory with experiment and the selected values of the surface tension coefficient α and the average radius of nanocrystals R_0 are shown in Fig. 6.

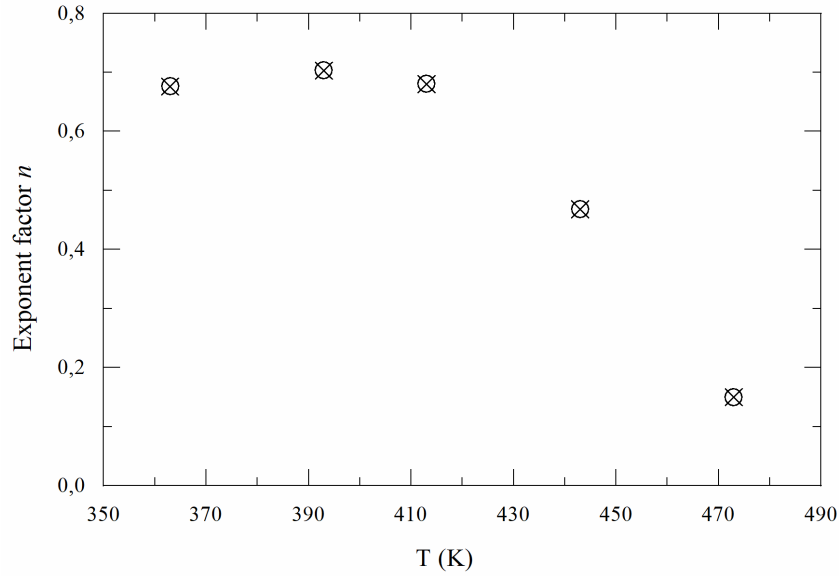


Fig. 5. The exponent factor of ac conductivity.

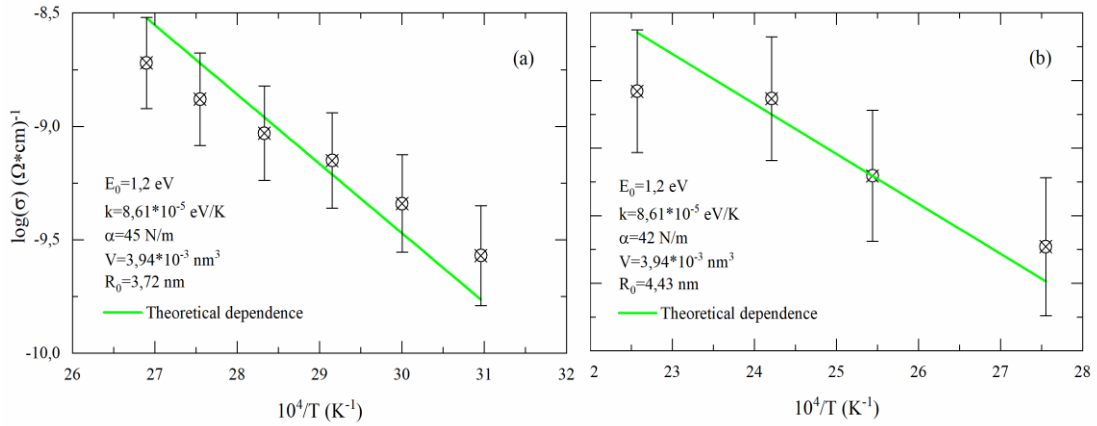


Fig. 6. Comparison of theory [5] with experiment for the temperature dependence of the ionic conductivity of the opal- $\text{NaBi}(\text{MoO}_4)_2:\text{Gd}^{3+}$ nanocomposite: $R_0 = 3.72$ nm (a) and $R_0 = 4.43$ nm (b).

The experimental points fit well with solid straight lines, which were constructed using formula (1) in different temperature ranges (Fig. 6 a, b). Thus, obtained values of the nanocrystal sizes $R_0 \approx 4$ nm confirm the hypothesis that nanocrystallization occurs on the surface of globules, which has its own substructure of the same scale, and surface details are the centers of nanocrystallization. In this case, the conductivity is predominantly of a surface nature. Ion hops occur on the surface of nanocrystals, on which there are increased concentration of impurities and structural defects including acid native vacancies, as well as vacancies in the disordered sublattice of Na^+ and Bi^{3+} ions. Additional internal deformations on the surface of nanocrystals arising due to surface tension forces lead to a decrease in the energy barriers for ion diffusion.

4. Conclusions

An increase in the ionic conductivity in the nanocrystalline state of the nonlinear insulator $\text{NaBi}(\text{MoO}_4)_2:\text{Gd}^{3+}$, which has a disordered sublattice of Na^+ and Bi^{3+} ions, in the opal- $\text{NaBi}(\text{MoO}_4)_2:\text{Gd}^{3+}$ nanocomposite was experimentally established. The increase

in ionic conductivity is due to an increase in the contribution of the surface conductivity of nanocrystals, for which, because of the action of surface tension forces, the diffusion activation energy decreases. Comparison with theory [5] made it possible to estimate the average size of nanocrystals in the nanocomposite. The obtained value correlates with the scale of the structure of the surface of silica globules, on which nanocrystallization occurs.

References

1. **Moiseienko, V.M.** Nanocomposites on the Base of Synthetic Opals and Nanocrystalline Phases of Bi-containing Active Dielectrics / V.M. Moiseienko, M.P. Derhachov, B. Abu Sal, R. Holze, M. Brynza // Springer Proceedings in Physics. – 2017. – Vol. 50 (195). – P. 661 – 674.
2. **Derhachov, M.P.** Structure, Optical and Electric Properties of Opal-Bismuth Silicate Nanocomposite / M.P. Derhachov, V.M. Moiseienko, N.O. Kutseva, B. Abu Sal, R. Holze, S.M. Pliaka, A.V. Yevchyk // Acta physica polonica A. – 2018. – Vol. 133(4). – P. 847 – 850.
3. **Derhachov, M.P.** Fabrication and characterization of crystalline Bi_2TeO_5 – $\text{Bi}_4\text{Si}_3\text{O}_{12}$ – SiO_2 nanocomposite / M.P. Derhachov, V.M. Moiseienko, N.O. Kutseva, B. Abu Sal, R. Holze // Eur. Phys. J. Plus – 2019. – Vol. 134.
4. **Boyko, Y.I.** Poverkhnostnaya strukturnaya relaksatsiya i plastichnost' nanokristallov / Y. I. Boyko, V. F. Korshak // VANT. – 2015. – Vol. 5(99) – P. 77 – 80.
5. **Glinchuk, M.D.** Osobennosti ionnoy provodimosti kisloroda v oksidnoy nanokeramike / M. D. Glinchuk, P. I. Bykov, B. Khilcher // Fizika tverdogo tela. – 2006. – Vol. 48 (11). – P. 2079 – 2084.
6. **Kosacki, I.** Microstructure – Property relationships in nanocrystalline oxide thin films / I. Kosacki, H. U. Anderson // Ionics. – 2000. – Vol. 6. – P. 294 – 311.
7. **Ryadun, A.A.** EPR i fotolyuminesentsiya kristallov $\text{NaBi}(\text{MoO}_4)_2$, aktivirovannykh ionami gadoliniya / A.A. Ryadun, V.A. Nadolinnyy, B.N. Tsydypova, A.A. Pavlyuk // Fizika tverdogo tela. – 2015. – Vol. 57 (6). – P. 1168 – 1171.
8. **Koleschnichenko, K.A.** Pryzhkovaya provodimost' v kristallakh $\text{NaBi}(\text{MoO}_4)_2$ / K.A. Koleschnichenko, S.G. Korkin, A.Y. Kudzin, T.M. Stolpakova, Y.V. Gontarenko // Fizika tverdogo tela. – 1991. – Vol. 33 (3). – P. 751 – 754.
9. **Stöber, W.** Controlled growth of monodisperse silica spheres in the micron size range. / W. Stöber, A. Fink, E. Bohn // J Colloid Interface Sci. – 1968 – Vol. 26 (2) P. 62 – 69.
10. **Tsydypova, B.N.** Vyrashchivaniye kristallov dvoynogo molibdata $\text{NaBi}(\text{MoO}_4)_2$ / B.N. Tsydypova, A.A. Pavlyuk, Y.V. Polyakova, A.I. Syprykin // Khimiya i khimicheskaya tekhnologiya. Fundamental'nyye problemy sozdaniya novykh materialov i tekhnologiy. – 2001. – Vol. 48 (9) – 1058 – 1061
11. **Moiseyenko, V.M.** Raman spectra of acoustooptic $\text{NaBi}(\text{MoO}_4)_2$ / V.M. Moiseyenko, Y.I. Bogatirjov, A.M. Jeryemenko // J Raman Spectroscopy. – 2000. – Vol. 31. – P. 539 – 541.
12. **Dovbeshko, G.** Vibrational spectra of opal-based photonic crystals / G. Dovbeshko, O. Fesenko, V. Boyko, V. Romanyuk, V. Moiseyenko, V. Gorelik, L. Dolgov, V. Kiisk, I. Sildos // IOP Conf. Series: Materials Science and Engineering – 2012. – Vol. 38.
13. **Iveronova, V.I.** X-ray scattering theory / V. I. Iveronova, G. P. Revkevich // Moscow: Ed. Moscow State University. – 1978. – Vol. 277.
14. **Jonscher, A.K.** Dielectric relaxation in solids. – J. Phys. D. Appl. Phys. – 1999. – Vol. 32.
15. **Elliott, S.R.** A.c. conduction in amorphous chalcogenide and pnictide semiconductors. – 1987. – Adv. Phys. – Vol. 36. – P. 135 – 217.